Peripheral Refraction Validity of the Shin-Nippon SRW5000 Autorefractor

Running Title: Validity of peripheral autorefraction with SRW-5000

Authors: Uchechukwu L. Osuagwu MSc, OD[*]

Marwan Suheimat PhD[*]

James S. Wolffsohn PhD FAAO[†]

David A. Atchison DSc FAAO[*]

Author Affiliations: [*]Institute of Health and Biomedical Innovation, Queensland University of Technology, Brisbane, 4059, Australia

[†]Ophthalmic Research Group, Life and Health Sciences, Aston University, Birmingham, United Kingdom

Corresponding Author: Uchechukwu L. Osuagwu

Email: uchechukwulevi.osuagwu@hdr.qut.edu.au

Number of Tables: 0

Number of figures: 9

Submission Date: 25/11/2015

Date of Acceptance: 10/04/2016

Abstract

Purpose: To investigate the operation of the Shin-Nippon/Grand Seiko autorefractor and whether higher-order aberrations affect its peripheral refraction measurements.

Methods: Information on instrument design, together with parameters and equations used to obtain refraction, was obtained from a patent. A model eye simulating the operating principles was tested with an optical design program. Effects of induced defocus and astigmatism on the retinal image were used to calibrate the model eye to match the patent equations. Coma and trefoil were added to assess their effects on the image. Peripheral refraction of a physical model eye was measured along four visual field meridians with the Shin-Nippon SRW-5000 and a Hartmann-Shack aberrometer, and simulated autorefractor peripheral refraction was derived using the Zernike coefficients from the aberrometer.

Results: In simulation, the autorefractor's square image was changed in size by defocus, into rectangles or parallelograms by astigmatism, and into irregular shapes by coma and trefoil. In the presence of 1.0 D oblique astigmatism, errors in refraction were proportional to the higher-order aberrations, with up to 0.8 D sphere and 1.5 D cylinder for ±0.6 μm of coma or trefoil coefficients with a 5 mm diameter pupil. For the physical model eye, refraction with the aberrometer was similar in all visual field meridians, but refraction with the autorefractor changed more quickly along one oblique meridian and less quickly along the other oblique meridian, than along the horizontal and vertical meridians. Simulations predicted that higher-order aberrations would affect refraction in oblique meridians, and this was supported by experimental measurements with the physical model eye.

Conclusions: The autorefractor's peripheral refraction measurements are valid for horizontal and vertical field meridians, but not for oblique field meridians. Similar instruments must be validated before being adopted outside their design scope.

Keywords: Shin-Nippon/Grand Seiko autorefractor; peripheral refraction; COAS-HD aberrometer; higher-order aberrations; Hartmann-Shack aberrometer.

Open-view automated autorefractors offer a binocular open-field of view during objective measurement of central refraction. The open-view makes it easy to view targets at a range of locations and the lack of internal fixation target or enclosed view minimizes the influence of proximal accommodation.[1-5] Grand Seiko autorefractors (Grand Seiko Co, Hiroshima, Japan), are open-view autorefractors which have also been marketed under the trade name Shin-Nippon (Ryusyo Industrial Co. Ltd., Osaka, Japan).

In the last decade there has been considerable interest in measuring peripheral (off-axis) refraction because of the possibility that it plays a role in the development of myopia.[5-9] These instruments are used widely for measuring peripheral refraction.[8, 10-14] However little, if any, attention has been given to the possibility that these refractions are invalid because of the influence of peripheral higher-order aberrations such as coma and trefoil.[15] Higher-order aberrations are present in small magnitudes during on-axis measurements, but increase away from fixation.[16-23] For example, for a 5 mm pupil the mean coma coefficient $\boldsymbol{C_3^1}$ increases linearly with field angle from a mean of 0.06 µm on-axis to 0.24 µm and 0.34 µm at 20° and 30° degrees, respectively, along the horizontal visual field meridian.[18]

Shin-Nippon autorefractors operate on the image size principle in which refraction is linearly related to angular size of the retinal image. A literature review yielded basic information on the image size principles used by Shin-Nippon autorefractors.[3, 24, 25] A patent search yielded four relevant Japanese patents, with patent JP11332827A providing information about operating principles including measured parameters and equations for obtaining refraction components.[26] This study uses an examination of this patent, modelling simulations and measurements with a physical model eye to investigate the operation principles of the Shin-

Nippon SRW-5000 autorefractor and whether higher-order aberrations influence its peripheral refraction measurements.

Methods

Overview

The operation principles of the Shin-Nippon SRW-5000 autorefractor described in a patent were verified in the laboratory with a simple physical model eye and simulated with a theoretical model eye in an optical design program. The laboratory measurements and simulations allowed determination of the constants and the unit used for angles in instrument equations. The simulations were used to mimic the effects of aberrations on the image formed by the autorefractor and to predict its refraction in the presence of peripheral higher-order aberrations. The simulated predictions were compared with measurements with a second physical model eye mounted in front of a Shin-Nippon autorefractor and a commercial Hartmann-Shack aberrometer.

Principles of operation of Shin-Nippon SRW-5000 autorefractor

The autorefractor is formed from four main arms (see Fig. 1, Supplemental Digital Content 1). These are a light projection optical system which projects a square pattern into the eye, an exit path which re-images the pattern on a CCD array, a fixation target path which provides both a fixation target and illumination of the front of the eye, and an imaging optical system which overlays the front of the eye onto the same CCD array.[26] For the entrance path (Fig. 1A), two square masks (or in some cases four separate lines which could form a square if extended) create the measurement target. The light starting from a point *Q* passes near the edge of the pupil of the eye where it forms a square *K* in the pupil plane and proceeds to form image *T* on the retina. *a* is the horizontal length of *K*, *d* is the distance from the object to the image *K*, and d_0 is the distance from the pupil to the image. The exit path (Fig. 1B) contains a mirror with a hole in the middle conjugate with the centre of the eye pupil, allowing only light passing through or near the center of the eye pupil to be in the path and thus minimizing aberrations, to form image L on the CCD camera at a distance d_1 from the pupil. In effect, the instrument is a single pass system, in which the exit path has a negligible effect on aberrations. The instrument measures distances X_0 and Y_0 and angles β_1 and β_2 as explained in Fig. 2, and calculates sphere, cylinder and axis according to Eq.s (1-3):[26]

$$SPH = \frac{1}{4ad_1(1-\beta_1\beta_2)}\left\{X_0 + Y_0 \pm \sqrt{(X_0+Y_0)^2 + 4X_0Y_0\beta_1\beta_2}\right\} + \frac{1}{d} \quad (1)$$

$$CYL = \frac{\pm 1}{2ad_1(1-\beta_1\beta_2)}\sqrt{(X_0-Y_0)^2 + 4X_0Y_0\beta_1\beta_2} \quad (2)$$

$$AXIS = \frac{1}{2}\tan^{-1}\frac{2Y_0\beta_2}{X_0-Y_0} \quad (3)$$

Laboratory investigation

A setup was built in the laboratory to verify the effects of defocus and astigmatism on the target. A simple eye model, consisting of a 50 mm focal length lens placed at the position of the cornea (front surface radius of curvature = 33.55 mm) and graph paper for a retina, was mounted in front of the Shin-Nippon autorefractor with alignment using reflections of the alignment Light Emitting Diodes in the front surface of the lens. A telecentric camera was focused on the retina to monitor the retinal image (*T* in Fig. 1). The instrument display was used to monitor the size and shape of the image after a second passage through the eye. Defocus was introduced by moving the retina back and forth, and cylindrical error was introduced by placing cylindrical trial lenses in front of the model eye.

The 'retina' was removed and a variable focus camera was moved along the optic axis to obtain the images of the two masks in the projection path (see elements 7 and 5, Fig. 1, Supplemental Digital Content 1). The image of mask 5 came into focus at the back focal length of the 50 mm lens (the retinal plane), while the image of mask 7 came into focus 16.667 mm behind the 50 mm lens (one third of the distance between the cornea and the retina). Images *T* and *L* (Fig. 1) were affected as described in the patent and measuring the sizes of the two mask images, masks 7 and 5 were calculated to be 1.5 mm x 1.5 mm and 3.0 mm x 3.0 mm, respectively, at their locations inside the instrument. Their locations within the instrument corresponded to the back focal point of lens 6 and front focal point of lens 2 for mask 5, and 25 mm to the left of lens 6 (half the focal length of lens 6) for mask 7. The value for *a*, being the side of the square target in the pupil plane (Fig. 1A), was measured as 3.0 mm.

Simulation for defocus and astigmatism calibrations

From the optical design in the patent and the laboratory investigation, the Shin-Nippon autorefractor was simulated in the optical design program Zemax (Zemax Optics Studio 15, LLC, Redmond, WA, USA) with a single refracting surface paraxial model eye. Defocus was introduced by moving the retina longitudinally. Horizontal/vertical astigmatism and oblique astigmatism were introduced by including C_2^2 and C_2^{-2} aberration coefficients, respectively, in a phase plate at the lens. From various amounts of defocus, X_0, Y_0, β_1 and β_2 in image *L* were measured with a tool available in Zemax and used to determine constants d_1 and d given *a* (measured experimentally in the previous section) in Eq.s 1-3 and for the simulation as –0.0252 mm and 0.0084 mm. Manipulating astigmatism confirmed the constants and showed that angles used in eq. (2) were in radians. Eq. (1) converged only when the sign in $(X_0 + Y_0)^2$ was made negative, so that the equation became:

$$SPH = \frac{1}{4ad_1(1-\beta_1\beta_2)}\left\{X_0 + Y_0 \pm \sqrt{(X_0 - Y_0)^2 + 4X_0Y_0\beta_1\beta_2}\right\} + \frac{1}{d} \qquad (4)$$

The error in sign in eq. (1) was probably a typographical error. Negative cylinders were used during the astigmatism calibration, which required –1 rather than +1 in the numerator of eq. (2) and the positive rather than the negative root in eq. (4).

Starting with an emmetropic eye, a smaller image L occurred when hyperopia (negative defocus) was simulated and a larger image occurred when myopia (positive defocus) was simulated. Vertical/horizontal astigmatism changed the image L from a square to a rectangle, and oblique astigmatism changed the square to a parallelogram (Fig. 2A). The center of L was determined as the intersection of the diagonals drawn across the image. X_0 was the horizontal distance through the center of the image between the outer edges of the left and right bars, and Y_0 was the vertical distance through the center of the image between outer edges of the top and bottom bars. The angles β_1 and β_2 were measured from the x, y coordinate points (x_1, y_1,), (x_2, y_2) and (x_3, y_3) as:

$$\beta_1 = \tan^{-1}[(y_1 - y_2)/(x_1 + x_2)],\ \beta_2 = \tan^{-1}[(x_1 - x_3)/(y_1 + y_3)] \qquad (5)$$

Simulating effects of higher-order aberrations on peripheral refraction

The effects of higher-order aberrations were predicted using the Zemax simulation. Different amounts of vertical coma, horizontal coma, oblique trefoil and trefoil were induced on the phase plates of the Zemax model eye (described in the section for calibration) through their Zernike coefficients C_3^{-1}, C_3^{1}, C_3^{-3} and C_3^{3}, respectively, in magnitudes not exceeding 0.6 µm (as might be present at ±20° along the horizontal visual field meridian in eyes with 5 mm pupil diameter in young adult myopes)[18]. Coma and trefoil caused similar, irregular changes to the image L. Fig. 2B shows the effect of coma. Similar to astigmatism, dimensions and angles were determined for image L, and parameters were substituted into Eq.s (2) and (4) to calculate refraction. Coma and trefoil did not influence refraction in the presence of defocus or vertical/horizontal astigmatism because one of the angles β_1 and β_2 was not affected. Therefore, the higher-order aberrations were simulated in the presence of +1.00 D oblique astigmatism C_2^{-2}.

Effects of higher-order aberrations on peripheral refraction of a physical model eye

Effects of higher-order aberrations on peripheral refraction were determined using a physical model eye made by Shen and Thibos.[27] Refraction was obtained with a COAS-HD aberrometer (Complete Ophthalmic Analysis System - High Definition, Wavefront Sciences Inc., Albuquerque, USA) and a SRW-5000 Shin-Nippon autorefractor in 5° steps along 4 visual field meridians. The purposes of the COAS-HD were firstly to provide refractions that should not be influenced by the meridional effects described in the previous section, and to determine higher-order aberrations of the physical model eye to be used in simulations. To match the pupil size used by the autorefractor to calculate refraction, sphere and cylinder refraction of the COAS-HD aberrometer were calculated from second- and fourth-order Zernike coefficients for a 4.5 mm pupil.

The eye was mounted in a cage mount, in the usual place of a right eye in front of each instrument, and attached to two goniometers. One goniometer allowed eye rotation along the horizontal meridian in 1° steps. The second goniometer was situated near the cage mount and allowed eye rotation along vertical and oblique meridians in 2° steps. In order to obtain measurements along oblique meridians (45°-225° and 135°-315°) and to be able to swap between them, a post mounting angle block and an angle clamp were added to the attachment to tilt the eye by 45°. To change between the 45°-225° and 135°-315° meridians, the added components were rotated by 180°. Reliable measurements were obtained with the model eye to 30° and 40° from fixation with the COAS-HD aberrometer and autorefractor, respectively. Beyond 30° the corneal reflections used for alignment with the autorefractor were not visible. For each field location, two and six measurements were taken with the COAS-HD, and autorefractor, respectively. Refractions were averaged by a vector method.[28] Angle convention was taken from the examiner's perspective. Positive angles horizontally were taken as rotation of the eye to the left (nasal visual field), positive angles vertically were taken as rotation of the eye downwards (superior visual field), and visual field meridians were specified by rotation anticlockwise from the examiner's right side.

The Zernike coefficients obtained from the COAS were entered into the Zemax simulation to determine the contribution of different aberrations to the error in Shin-Nippon measurement. This was done both with and without higher-order aberration coefficients of coma and trefoil to test their effects on the refraction.

Results

Effects of coma and trefoil on simulated Shin-Nippon refraction

Similar magnitudes of coma and trefoil caused similar refraction errors (see Fig. 2, Supplemental Digital Content 1). For 1.0 D of oblique astigmatism, the errors were affected linearly by coma coefficient and reached 0.8 D of sphere and 1.5 D of cylinder over the coefficient range –0.6 µm to +0.6 µm Essentially the error was 1.0 D astigmatism per micrometer of aberration coefficient. For coma coefficients greater than +0.4 µm, angles β_1 and β_2 had opposite signs which led to failure in calculating refraction results using eq.s (2) and (4).

Aberration coefficients and peripheral refractions of the physical model eye

Higher order aberration in the peripheral field was dominated by coma, which had similar rates of change along all meridians at approximately 0.021 µm per degree of visual field angle (see Fig. 3, supplemental Digital Content 1). By comparison, trefoil was small and changed slowly with visual field angle.

Fig. 3 shows sphere and cylinder refraction components along horizontal, vertical and oblique meridians with the COAS-HD aberrometer to ±40° and the Shin-Nippon SRW-5000 autorefractor to ±30° eccentricity. For the COAS-HD, the sphere became more positive from the center to the periphery, while the cylinder became highly negative (more negative peripheral cylinder with the autorefractor than with the aberrometer), with both showing quadratic relationships with field eccentricity. Refractions were similar along all meridians, except between –15 and –25º for the 45°-225° meridian where there was a negative dip in sphere. Tilting the plots slightly to improve symmetry, by raising them for negative angles and lowering them for positive angles, gave approximate sphere and cylinder of +1.0 D and –3.5 D at ±30°, respectively, and +2.0 D and –6.5 D at ±40º, respectively. With the Shin-Nippon autorefractor, results were again similar along the horizontal and vertical field meridians with sphere and cylinder being approximately 0 D and –4.5 D, respectively, at ±30°. Compared with these, refraction changes were high for the 45°-225° meridian (cylinder to –5.5 D) and low for the 135°-315° meridian (cylinder to –3.0 D).

Fig. 4 shows sphere and cylinder refraction components along the four meridians, with simulations derived from COAS-HD derived coefficients and the experimental results with the Shin-Nippon SRW-5000 autorefractor (the latter the same as for Fig. 3). The simulation had similar values along the horizontal, vertical and 135°-315° meridians, with changes in sphere and cylinder from the center to the edge of the field (±40°) of +3.5 D and –5.5 D, respectively. However, there was considerable asymmetry for the 45°-225° meridian with the cylinders having relative low values to –4 D for negative angles and high values to –9 D for positive angles.

Compared with the simulation, experimental cylinders with the Shin-Nippon autorefractor were shifted in the negative direction for cylinders (Fig. 4). Again, horizontal and vertical field meridians were similar. The asymmetries in the simulation for the 45°-225° meridian did not occur experimentally.

When higher-order aberrations were removed from the simulation (Fig. 5), there was little effect for the horizontal, vertical and 135°-315° meridians, but the asymmetry was considerably reduced along the 45°-225° meridian. The changes in sphere and cylinder refractions along the 45°-225° meridian reached –2.6 D and +3.0 D, respectively (Fig. 6).

Discussion

The principles by which the Shin-Nippon/Grand Seiko Autorefractor SRW-5000 determines the refractive error components were replicated. The units of the constants and angles used in the instrument equations for calculating refraction and refraction errors were determined, with the angles β_1 and β_2 being specified in radians, and eq. (4) yielding the expected sphere and cylinder values in the absence of higher-order aberrations. Coma and trefoil caused non-quadrilateral changes in the image which were not mentioned in the patent.[26] Angles β_1 and β_2 were altered depending on the coefficients of coma and trefoil. Higher-order aberrations of coma and trefoil caused theoretical errors in the autorefractor sphere and cylinder measurements in the presence of oblique astigmatism, amounting to 1.0 D astigmatism per micrometer of higher-order aberration coefficient in the presence of 1.0 D of oblique astigmatism with a 5 mm pupil.

A variety of determinations using a physical model eye indicated that the autorefractor refractions were affected by higher-order aberrations such that these refractions depended upon the visual field meridian (Figs. 3-6). The determinations included both simulations, based upon aberrations, and autorefractor measurements. For the simulations, the peripheral refraction along the horizontal and vertical meridians was hardly affected by higher-order aberrations, peripheral refraction along the 135°-315° meridian was only slightly affected, and peripheral refraction along the 45°-225° meridian was affected considerably. The main higher-order aberrations affecting refraction were the comas, which varied approximately linearly with visual field angles (see Fig. 3, supplementary Digital Content 1).

There was considerable discrepancy in peripheral refraction between the autorefractor simulations and the experimental results along the 45°-255° meridian (e.g. Fig. 4): The asymmetry between the positive and negative sides of the visual field in the simulation for

45°-255° meridian did not occur experimentally. This could be due to the method used in our simulation: we used a square mask in the simulations whereas the instrument uses horizontal and vertical bars. The instrument uses a scanning technique in detecting the dimension X_0, Y_0 and the angles β_1, β_2 which may reduce the effects of higher-order aberrations. We think that the instrument uses a cross correlation matrix whereby predetermined square bars are designed to scan across the image L horizontally, vertically and rotationally in search of regions with the highest correlations in each of the scanning directions.

The coma in the model eye was high relative to that reported for most real eyes in our previous investigations.[17, 19, 22, 23] For a small group of older adults (mean age 63 years), Mathur, and Atchison[23] found a mean rate of change of coma of 0.018 µm/° for elliptical pupils with a major axis diameter of 5 mm, which is similar to the model eye of approximately 0.020 µm/° for a 4.5 mm circular pupil, and so the coma for the model eye is realistic. While coma was the only higher-order aberration that was of consequence for affecting refraction along oblique meridians of the model eye, it is possible that some real eyes have high levels of trefoil that would influence peripheral refraction.

The majority of previous studies on peripheral refraction with Shin-Nippon/Grand Seiko autorefractors have investigated along the horizontal visual field meridian, with few studies investigating along the vertical field meridian[12, 29] and only one study considering oblique meridians.[13] Our results indicate that peripheral refraction measurements with the Shin-Nippon SRW-5000 are valid along horizontal and vertical visual field meridians, but are not valid along oblique meridians in people with high levels of peripheral coma.

Other versions of the Shin-Nippon autorefractors have different features than those of the instrument used in this study. The main variations between different versions of the Shin-Nippon autorefractor are in target shape and size. The earliest version of the Shin Nippon autorefractors was marketed as the Grand Seiko WV-500K.[7,30] It projected a complete circle rather than the square used by the SRW-5000. The projected image was changed after it was found to be in breach of a patent.[31] Other than the projected image, the mechanisms of operation are similar for the different Shin Nippon/Grand Seiko autorefractors.[30-32] The Grand Seiko WAM-5500 and the NVision K-5001, the latest version also marketed as Grand Seiko WR-5100K, reduce the necessary pupil size to 2.3 mm, use a smaller infrared measurement ring and incorporate a keratometer.[3, 4, 33] While the present work is relevant to the newest instrument, a smaller pupil is likely to be less influenced by higher-order aberrations. To investigate the effects of the projected circular ring on peripheral refraction measurements, additional work was carried out in our laboratory using the newest Shin Nippon/Grand Seiko autorefractor (NVision K-5001). The method was the same as for measurements with the SRW-5000 autorefractor. Peripheral refraction measured along the four visual field meridians of the Thibos physical model eye showed that the instrument gave unreliable results in all but the horizontal meridian. For the vertical and oblique meridians, results were not reproducible, which we attribute to alignment difficulties with the new instrument. In the older instrument, the internal target was kept on to monitor the changes that occur to the peripheral image,[30] but this was not available in the new instrument.[32]

In summary, the angles used by the Shin-Nippon/Grand Seiko autorefractor SRW-5000 in calculating refraction are designated in radians and equations for calculating refraction, are valid. Defocus and astigmatism cause regular changes in the image used for determining refractions, while coma and trefoil cause irregular changes in this image. Higher-order aberrations such as coma and trefoil can affect refraction in oblique meridians of the visual field, particularly the 45°-225° meridian. We advise that the instrument should not be used for peripheral refraction along these meridians and similar instruments must be validated before being adopted outside their design scope.

Acknowledgements

This work was supported by Australian Research Council Discovery grants DP110102018 and DP140101480 to David Atchison. Uchechukwu Osuagwu was supported by a postgraduate scholarship from the School of Optometry and Visual Science at Queensland University of Technology. We thank Larry Thibos for the loan of his model eye.

Disclosure Statement: The authors report no conflicts of interest and have no proprietary interest in any of the materials mentioned in this article. The manuscript was presented as a paper "Validity of peripheral refraction, using the Shin-Nippon/Grand Seiko autorefractor" at the American Academy of Optometry annual meeting, October 7, New Orleans, LA, USA.

References

1. Hung GK, Ciuffreda KJ, Rosenfield M. Proximal contribution to a linear static model of accommodation and vergence. Ophthalmic Physiol Opt 1996;16:31-41.

2. Rosenfield M, Ciuffreda KJ. Effect of surround propinquity on the open-loop accommodative response. Invest Ophthalmol Vis Sci 1991;32:142-7.

3. Davies LN, Mallen EAH, Wolffsohn JS, Gilmartin B. Clinical evaluation of the Shin-Nippon NVision-K 5001/Grand Seiko WR-5100K autorefractor. Optom Vis Sci 2003;80:320-4.

4. Sheppard AL, Davies LN. Clinical evaluation of the Grand Seiko Auto Ref/Keratometer WAM5500. Ophthalmic Physiol Opt 2010;30:143-51.

5. Moore KE, Berntsen DA. Central and peripheral autorefraction repeatability in normal eyes. Optom Vis Sci 2014;91:1106-12.

6. Hoogerheide J, Rempt F, Hoogenboom WPH. Acquired myopia in young pilots. Ophthalmologica 1971;163:209-15.

7. Fedtke C, Ehrmann K, Holden BA. A review of peripheral refraction techniques. Optom Vis Sci 2009;86:429-46.

8. Chen X, Sankaridurg P, Donovan L, Lin Z, Li L, Martinez A, Holden B, Ge J. Characteristics of peripheral refractive errors of myopic and non-myopic Chinese eyes. Vision Res 2010;50:31-5.

9. Sankaridurg P, Holden B, Smith E, Naduvilath T, Chen X, de la Jara PL, Martinez A, Kwan J, Ho A, Frick K. Decrease in rate of myopia progression with a contact lens designed to reduce relative peripheral hyperopia: one-year results. Invest Ophthalmol Vis Sci 2011;52:9362-7.

10. Radhakrishnan H, Charman WN. Peripheral refraction measurement: does it matter if one turns the eye or the head? Ophthalmic Physiol Opt 2008;28:73-82.

11. Kang P, Gifford P, McNamara P, Wu J, Yeo S, Vong B, Swarbrick H. Peripheral refraction in different ethnicities. Invest Ophthalmol Vis Sci 2010;51:6059-65.

12. Atchison DA, Pritchard N, Schmid KL. Peripheral refraction along the horizontal and vertical visual fields in myopia. Vision Res 2006;46:1450-8.

13. Ehsaei A, Mallen EAH, Chisholm CM, Pacey IE. Cross-sectional sample of peripheral refraction in four meridians in myopes and emmetropes. Invest Ophthalmol Vis Sci 2011;52:7574-85.

14. Berntsen DA, Mutti DO, Zadnik K. Validation of aberrometry-based relative peripheral refraction measurements. Ophthalmic Physiol Opt 2008;28:83-90.

15. Atchison DA. The Glenn A. Fry Award Lecture 2011: Peripheral optics of the human eye. Optom Vis Sci 2012;89:954-66.

16. Baskaran K, Theagarayan B, Carius S, Gustafsson J. Repeatability of peripheral aberrations in young emmetropes. Optom Vis Sci 2010;87:751-9.

17. Mathur A, Atchison DA, Scott DH. Ocular aberrations in the peripheral visual field. Opt Lett 2008;33:863-5.

18. Lundström L, Gustafsson J, Unsbo P. Population distribution of wavefront aberrations in the peripheral human eye. J Opt Soc Am A 2009;26:2192-8.

19. Mathur A, Atchison DA, Charman WN. Myopia and peripheral ocular aberrations. J Vis 2009;9.15:1-12.

20. Charman WN, Mathur A, Scott DH, Hartwig A, Atchison DA. Specifying peripheral aberrations in visual science. J Biomed Opt 2012;17:250041-9.

21. Fedtke C, Ehrmann K, Falk D, Bakaraju RC, Holden BA. The BHVI-EyeMapper: Peripheral refraction and aberration profiles. Optom Vis Sci 2014;91:1199-207.

22. Mathur A, Atchison DA, Neil Charman W. Effects of age on peripheral ocular aberrations. Opt Express 2010;18:5840-53.

23. Mathur A, Atchison DA, Charman WN. Effect of accommodation on peripheral ocular aberrations. J Vis 2009;9.20:1-11.

24. Mallen EAH, Gammoh Y, AlBdour M, Sayegh FN. Refractive error and ocular biometry in Jordanian adults. Ophthalmic Physiol Opt 2005;25:302-9.

25. Atchison DA. Comparison of peripheral refractions determined by different instruments. Optom Vis Sci 2003;80:655-60.

26. Masakatsu I. Eye refraction measuring apparatus and eye refraction measuring method. Japan patent JP11332827. 1999 28 May 1998. Available at: http://www.j-tokkyo.com/1999/A61B/JP11332827.shtml. Accessed July 1, 2014.

27. Shen J, Thibos LN. Measuring ocular aberrations and image quality in peripheral vision with a clinical wavefront aberrometer. Clin Exp Optom 2009;92:212-22.

28. Thibos LN, Wheeler W, Horner D. Power vectors: an application of Fourier analysis to the description and statistical analysis of refractive error. Optom Vis Sci 1997;74:367-75.

29. Berntsen DA, Mutti DO, Zadnik K. Study of theories about myopia progression (STAMP) design and baseline data. Optom Vis Sci 2010;87:823-32.

30. Wolffsohn JS, Gilmartin B, Mallen EAH, Tsujimura S. Continuous recording of accommodation and pupil size using the Shin-Nippon SRW-5000 autorefractor. Ophthalmic Physiol Opt 2001;21:108-13.

31. Wolffsohn JS, O'Donnell C, Charman WN, Gilmartin B. Simultaneous continuous recording of accommodation and pupil size using the modified Shin-Nippon SRW-5000 autorefractor. Ophthalmic Physiol Opt 2004;24:142-7.

32. Mallen EA, Gilmartin B, Wolffsohn JS, Tsujimura S. Clinical evaluation of the Shin-Nippon SRW-5000 autorefractor in adults: an update. Ophthalmic Physiol Opt 2015;35:622-7.

33. Bailey MD, Twa MD, Mitchell GL, Dhaliwal DK, Jones LA, McMahon TT. Repeatability of autorefraction and axial length measurements after laser in situ keratomileusis. J Cataract Refract Surg 2005;31:1025-34.

Figure legends

Fig. 1. Some of the optical set-up of the Shin-Nippon/Grand Seiko SWR-5000: A) Entrance path, B) Exit path. See text for details. Adapted from the patent.[26]

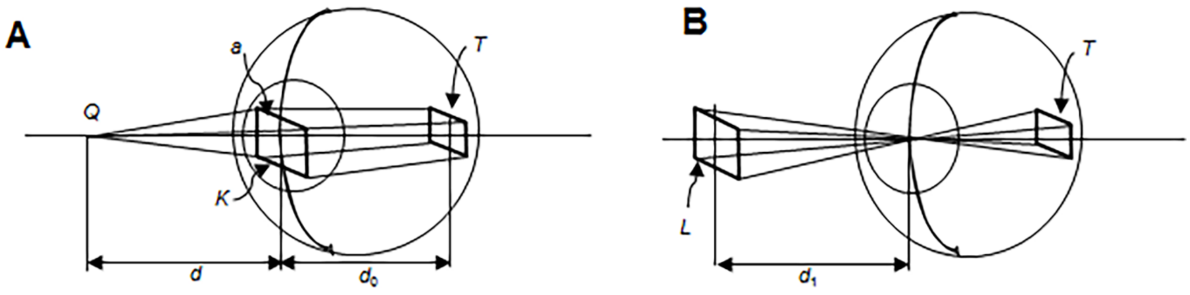

Fig. 2: Images *L*. X_0 and Y_0 image distances as determined from edge co-ordinates, and angles β_1 and β_2 when simulating A) 8 D oblique astigmatism with a 5 mm pupil, and B) +5.5 µm horizontal coma coefficient with a 5 mm pupil.

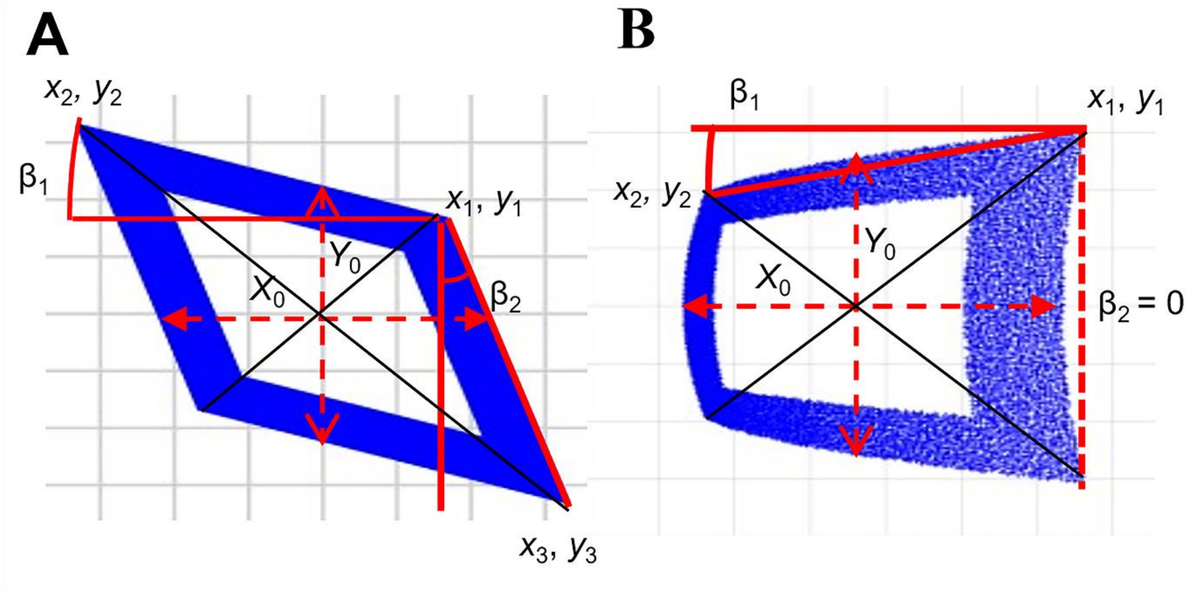

Fig. 3. Refraction of the physical model eye with the COAS-HD aberrometer and Shin-Nippon autorefractor, as a function of visual field angle, along A) horizontal, B) vertical, C) 45°–225° and D) 135°–315° visual field meridians, for a 4.5 mm pupil.

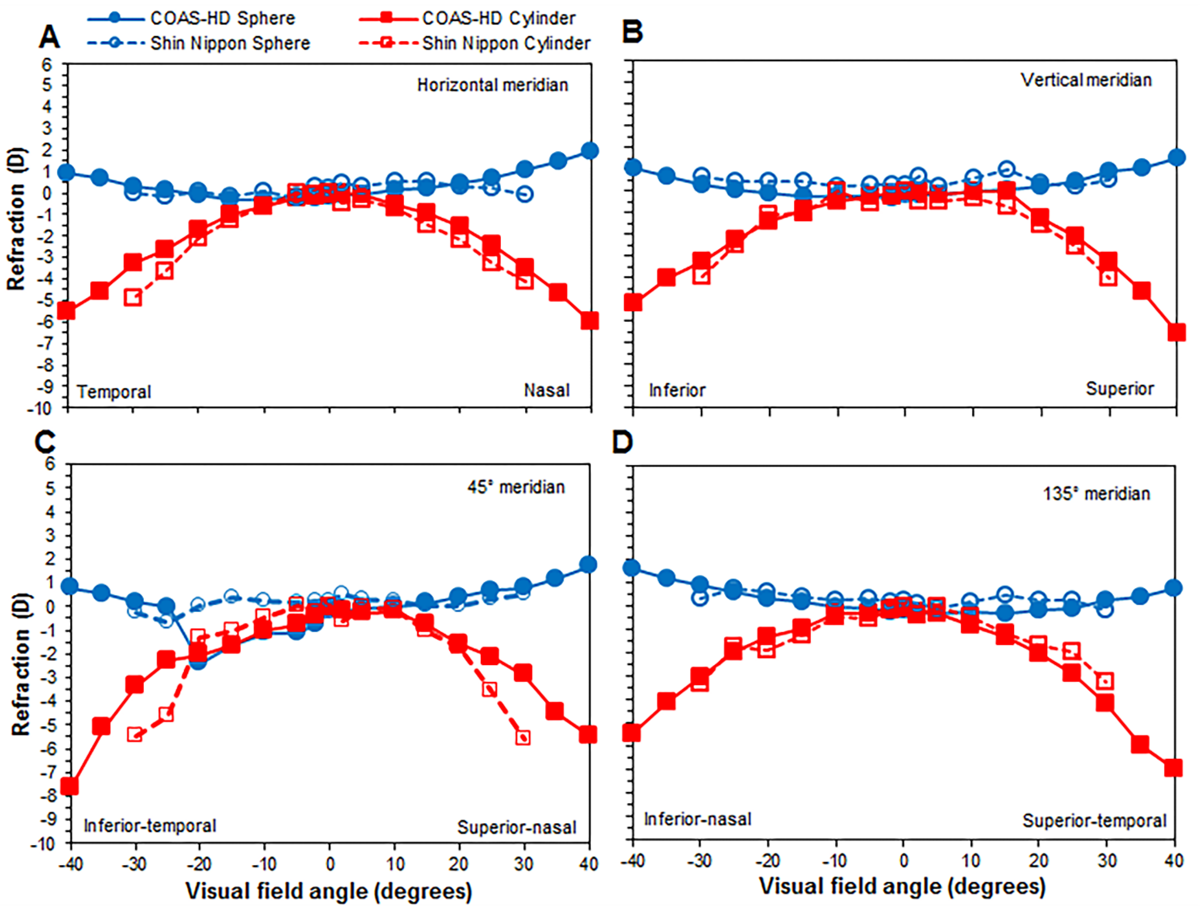

Fig. 4. Refraction of the physical model eye, determined from simulations using aberration coefficients derived from the aberrometer and measurement with the Shin-Nippon autorefractor, as a function of visual field angle, along A) horizontal, B) vertical, C) 45°–225° and D) 135°–315° visual field meridians, for a 4.5 mm pupil. The Shin-Nippon autorefractor results have been reproduced from Fig. 3.

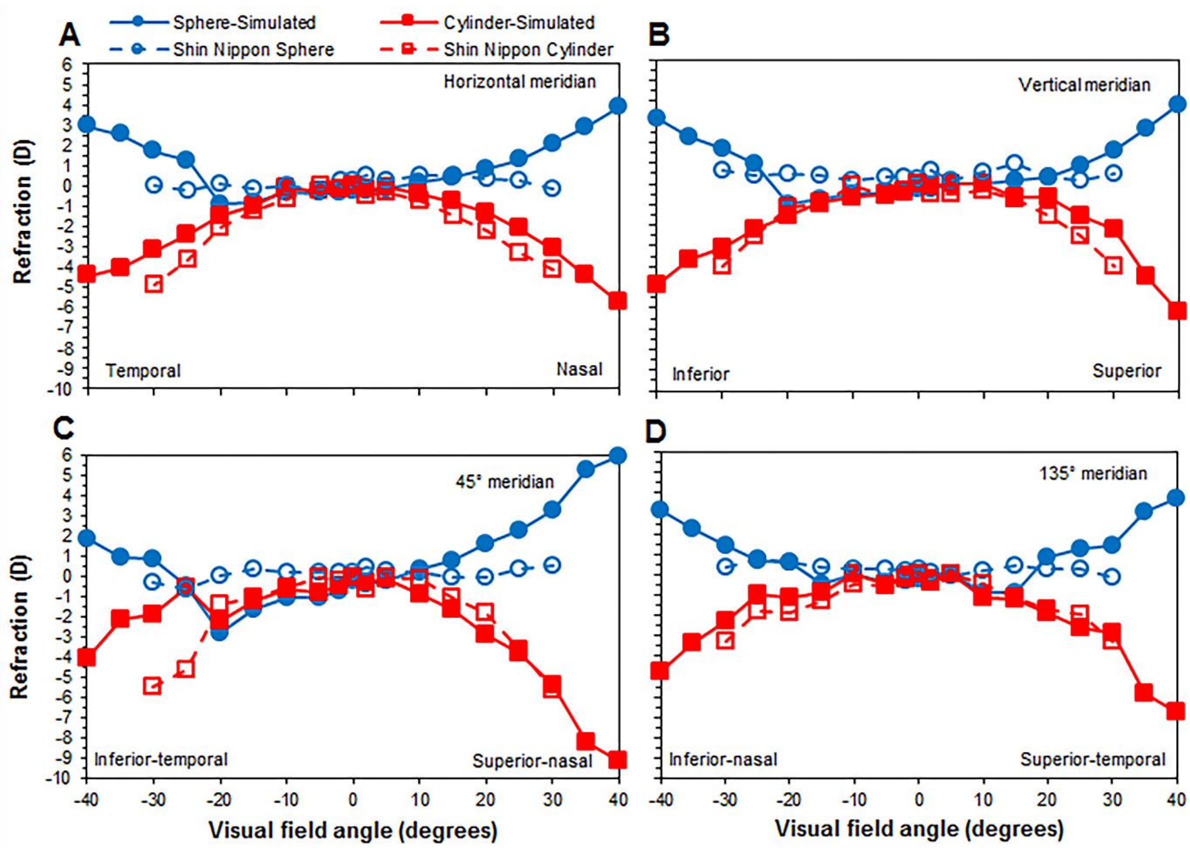

Fig. 5. Refraction of the physical model eye, determined from simulating the aberration coefficients derived from the aberrometer, as a function of visual field angle, along A) horizontal, B) vertical, C) 45°–225° and D) 135°–315° visual field meridians, for a 4.5 mm pupil. Simulations are done both with and without higher-order aberrations (the former are also shown in Fig. 4).

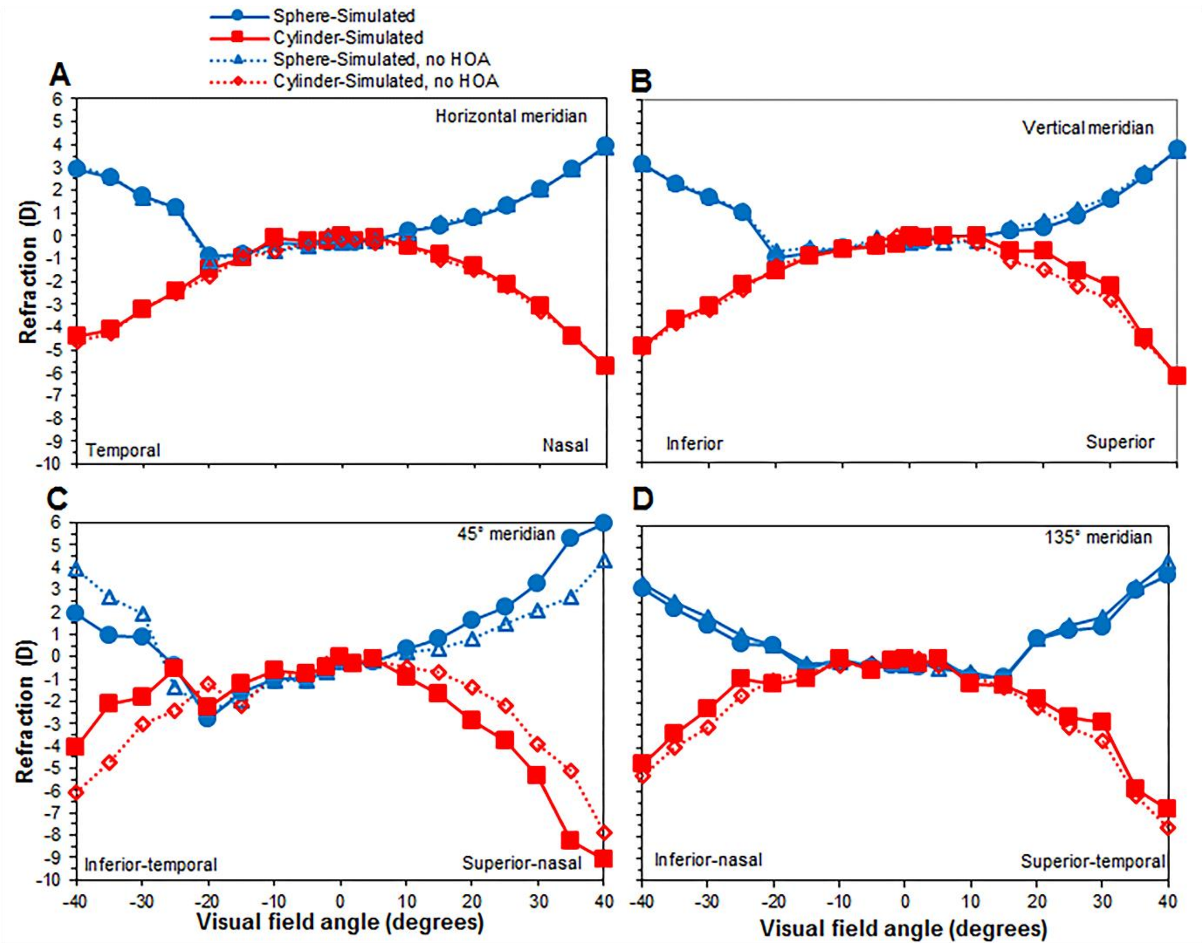

Fig. 6. Changes in simulated refraction when higher-order aberration (HOA) coefficients of the physical model eye are removed, as a function of visual field angle, along the A) horizontal and vertical and, B) 45°–225° and 135°–315° visual field meridians, for a 4.5 mm pupil.

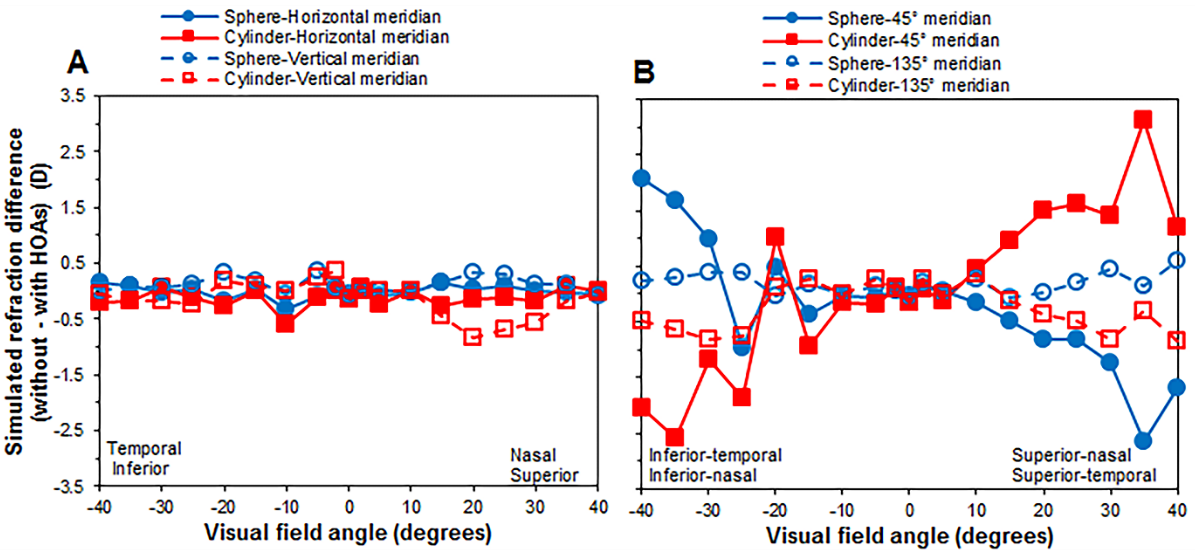

Supplementary Digital Content file for "Peripheral Refraction Validity of the Shin-Nippon SRW-5000 Autorefractor" by Osuagwu UL, Suheimat M, Wolffsohn JS, Atchison DA Optometry and Vision Science Volume 93, 2016

Fig. 1: Optical set-up of the Shin-Nippon/Grand Seiko SWR-5000 autorefractor. We thank Kenichi Omori from Rexxam Company Ltd. for permission to reproduce this figure from the patent (Masakatsu I. Eye refraction measuring apparatus and eye refraction measuring method. Japan patent JP11332827. 1999 28 May 1998. Available at: http://www.j-tokkyo.com/1999/A61B/JP11332827.shtml. Accessed July 1, 2014.).

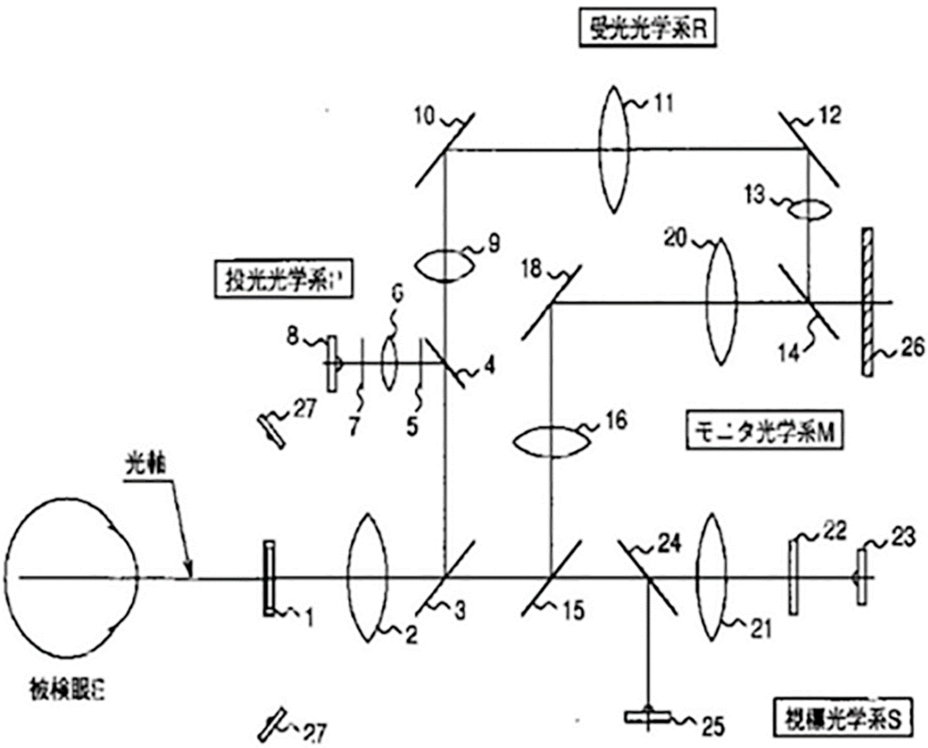

Fig. 2: Simulated errors in refraction as a function of coma coefficient with a 5 mm pupil: A) vertical coma in the presence of 1.0 D oblique astigmatism, B) horizontal coma in the presence of 1.0 D oblique astigmatism, and C) horizontal coma in the presence of 2.0 D oblique astigmatism. Doubling the oblique astigmatism from 1.0 D to 2.0 D increased the sphere and cylinder errors by about 40% and 10%, respectively.

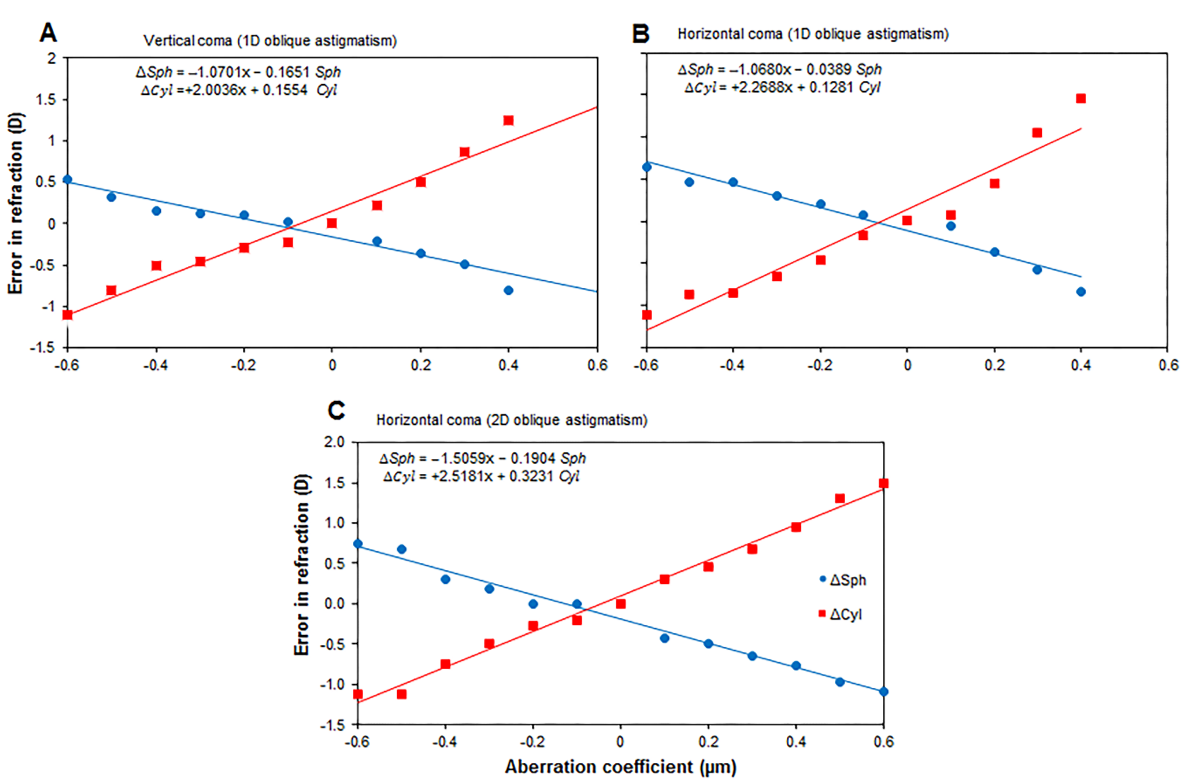

Fig. 3: Higher-order aberration coefficients of the Thibos physical model eye, measured with the COAS-HD aberrometer, as a function of visual field angle, along A) horizontal, B) vertical, C) 45°–225° and D) 135°–315° visual field meridians, for a 4.5 mm pupil. Rates of change of coma were similar along all meridians (when its horizontal and vertical components were combined) at approximately 0.021 µm per degree of visual field angle. By comparison, trefoil was small and changed slowly with visual field angle.